

Electron conductance of a cavity-embedded topological 1D chain

Danh-Phuong Nguyen, Geva Arwas, and Cristiano Ciuti

Université Paris Cité, CNRS, Matériaux et Phénomènes Quantiques, 75013 Paris, France

(Dated: March 1, 2024)

We investigate many-body topological and transport properties of a one-dimensional Su–Schrieffer–Heeger (SSH) topological chain coupled to the quantum field of a cavity mode. The quantum conductance is determined via Green’s function formalism in terms of the light-matter eigenstates calculated via exact diagonalization for a finite number of electrons. We show that the topology of the cavity-embedded many-electron system is described by a generalized electron-photon Zak marker. We reveal how the quantization of transport is modified by the cavity vacuum fields for a finite-size chain and how it is impacted by electronic disorder. Moreover, we show that electron-photon entanglement produces dramatic differences with respect to the predictions of mean-field theory, which strongly underestimates cavity-modified effects.

Introduction — In recent years there has been a growing interest in manipulating materials using cavity vacuum fields, as evidenced by various studies [1–4]. Various platforms, such as metallic split-ring terahertz electromagnetic resonators [5–7], and more recently, hyperbolic van der Waals materials [8], enable ultra-strong light-matter coupling due to their exceptional sub-wavelength photon mode confinement. On the theoretical front, several models have been proposed to study its impact on diverse aspects like superconductivity [9–11], quantum transport [12–15] and topology [16–22]. On the experimental front, this intricate physics has been demonstrated through investigations of magneto-transport properties [7], topological quantum Hall resistance [23], and critical temperature of a charge density wave transition [24] under strong light-matter interaction.

To address the challenges posed by the cavity quantum electrodynamics (QED) many-body problem, which involves both fermionic and bosonic particles, several approaches have been suggested in the literature. One such method is the adiabatic elimination, as suggested in Refs. [12, 13, 17, 21, 22]. In this approach, electronic states are coupled thanks to photon-mediated processes, resulting in an effective electronic Hamiltonian. However, it requires an energy scale separation between light and matter degrees of freedom, i.e., photon energy must be off-resonant to the relevant electronic transitions. Another viable approximation is the mean-field ansatz, initially proposed in Ref. [25] and then later used in Refs. [16, 26]. This technique works in the thermodynamic limit and it implies no entanglement between light and matter, allowing the ground state to be determined self-consistently through effective photon and electron Hamiltonians with renormalised parameters. However, this semi-classical regime overlooks quantum fluctuations and light-matter entanglement, possibly neglecting the potential emergence of interesting physics. For example, when light and matter are highly entangled, novel phenomena such as light-matter Chern numbers [19] and Majorana polaritons [20] can arise. This regime

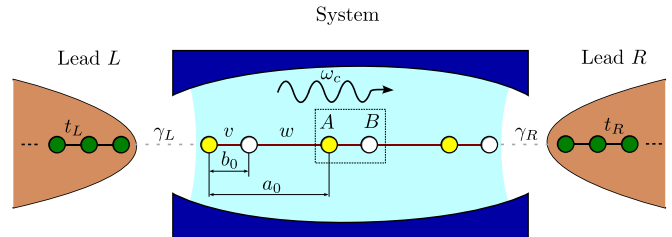


FIG. 1. Sketch of a cavity-embedded Su-Schrieffer-Heeger (SSH) chain, consisting of two sublattices A and B . The intra-cell (inter-cell) distance is a_0 (b_0). The corresponding electron hopping coupling is v (w). The cavity photon mode frequency is ω_c . The left (right) lead has hopping coefficient t_L (t_R), while its coupling to the system is γ_L (γ_R).

could be studied through bosonization of fermionic particles [14, 15], Density Matrix Renormalization Group (DMRG) [18, 20, 27], or exact diagonalization [19].

Up to now, to the best of our knowledge, no many-body topological markers have been investigated for cavity-embedded electron systems. Moreover, no exact results have been obtained for cavity-modified quantum transport for the many-electron case. In this article, we present a first theoretical investigation to address these two fundamental issues. We investigate the problem of a cavity-embedded Su-Schrieffer-Heeger (SSH) topological chain of finite length for a finite number of electrons. We show that the topology of this system is characterized by a many-body electron-photon Zak phase that generalizes the electronic marker introduced in [28, 29]. Moreover, we obtain exact results for the quantum conductance by a Green’s function formalism [30] by exploiting exact diagonalization results for the light-matter eigenstates. We show how the cavity vacuum fields can dramatically affect the transport, as well as a breakdown of mean-field theory due to sizeable electron-photon entanglement.

Cavity QED Hamiltonian — Let us consider the Hamiltonian describing an SSH chain with N unit cells

with two sublattices denoted as A and B (Fig 1):

$$\hat{\mathcal{H}}_{\text{SSH}} = v \sum_{n=1}^N \hat{c}_{n,B}^\dagger \hat{c}_{n,A} + w \sum_{n=1}^{N-1} \hat{c}_{n+1,A}^\dagger \hat{c}_{n,B} + \text{h.c.}, \quad (1)$$

where $\hat{c}_{n,\sigma}^\dagger$ creates an electron on the site n and sublattice $\sigma \in \{A, B\}$. Note that we have considered open boundary conditions for the chain. For simplicity, we will consider only one spin channel and omit the spin index. The intra-cell and inter-cell hopping amplitudes are denoted respectively as v and w . When $|v| > |w|$ the system is known to be topologically trivial, while $|v| < |w|$ gives a

$$\hat{\mathcal{H}}_S = \hbar\omega_c \hat{a}^\dagger \hat{a} + \left(v e^{-ig_v(\hat{a} + \hat{a}^\dagger)} \sum_{n=1}^N \hat{c}_{n,B}^\dagger \hat{c}_{n,A} + w e^{-ig_w(\hat{a} + \hat{a}^\dagger)} \sum_{n=1}^{N-1} \hat{c}_{n+1,A}^\dagger \hat{c}_{n,B} + \text{h.c.} \right). \quad (2)$$

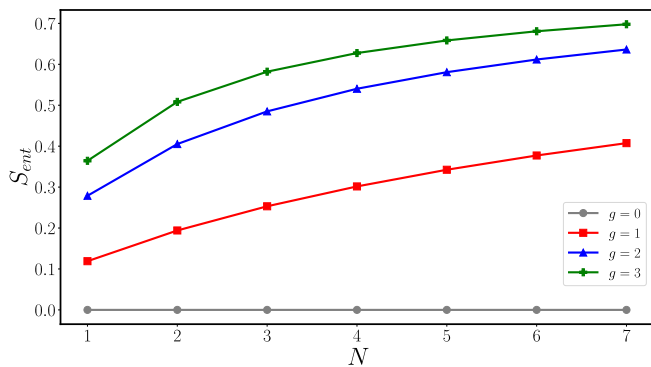


FIG. 2. Light-matter entanglement entropy as a function of system size N for the dimensionless light-matter coupling $g = 0, 1, 2, 3$. Other parameters: $w = \hbar\omega_c = v$, $b_0 = 0.5a_0$.

Let a_0 be the lattice constant and b_0 the intra-cell distance such that $0 \leq b_0/a_0 \leq 1$. Then, we can introduce dimensionless light-matter coupling constants $g_v = gb_0/a_0$ and $g_w = g(1 - b_0/a_0)$ where $g = eA_0a_0/\hbar$. In what follows, we will investigate finite-size chains and we will employ exact diagonalization techniques to determine exact results beyond the single-particle approximation and without adiabatic elimination of the photonic degrees of freedom.

Light-matter entanglement — In this and next section, we will consider the properties of the ground state (2), denoted as $|GS, N_e\rangle$, where N_e is the number of electrons. In particular we will focus on the physics at the half-filling point $N_e = N$. If one is interested in electronic observables, the key quantity is the electronic reduced density matrix formula obtained by tracing over the photonic degrees of freedom, namely $\hat{\rho}_{el}(N) = \text{Tr}_{\text{phot}}(|GS, N\rangle\langle GS, N|)$. Light-matter entan-

non-trivial topology with localised edge states and non-zero Zak phase at half-filling [28, 29]. For the photonic component, we consider a model describing a single-mode cavity with spatially homogeneous field described by the vector potential $\hat{\mathbf{A}} = A_0 \mathbf{u}(\hat{a} + \hat{a}^\dagger)$ where \hat{a}^\dagger (\hat{a}) represents the photonic creation (annihilation) operator, and \mathbf{u} is the orientation of the cavity mode polarization. For sake of simplicity, we will consider a linear polarization along the chain direction. We can express the vacuum field amplitude as $A_0 = \sqrt{\hbar\omega_c/2\epsilon_0 V_{\text{mode}}}$ where ω_c is the cavity frequency and V_{mode} the mode volume. Light-matter interaction can be introduced via the Peierls substitution giving the following cavity QED Hamiltonian:

glement can be then quantified by the entanglement entropy $S_{ent} = -\text{Tr}_{el}(\hat{\rho}_{el} \log \hat{\rho}_{el})$. In Fig. 2 we report the entanglement entropy as a function of system size N for different values of the light-matter coupling g . For increasing light-matter coupling, S_{ent} increases. We note that for a fixed coupling g the dependance on N tends to saturate for increasing N .

Many-body light-matter topological marker — For the case of a pure electronic system, a many-body topological Z_2 invariant has been introduced in Refs. [28, 29] by exploiting the concept of Resta's polarization $\hat{\mathcal{P}}$ [31]:

$$\hat{\mathcal{P}} = \exp\left(\frac{i2\pi}{N} \hat{R}\right), \quad (3)$$

$$\hat{R} = \sum_{n=1}^N n \hat{c}_{n,A}^\dagger \hat{c}_{n,A} + \left(n + \frac{1}{2}\right) \hat{c}_{n,B}^\dagger \hat{c}_{n,B},$$

where \hat{R} is the position operator. In Ref. [19] we have introduced the novel concept of an electron-photon Chern number which applies for 2D systems within the single-particle picture. For the present 1D many-body system, we have found the following topological light-matter marker:

$$Z^{(e-p)} = \frac{2}{\pi} \text{Im} \log \langle GS, N | \hat{\mathcal{P}} \otimes \hat{I}_p | GS, N \rangle, \quad (4)$$

$$= \frac{2}{\pi} \text{Im} \log \text{Tr}_{el}(\hat{\rho}_{el} \hat{\mathcal{P}}),$$

where \hat{I}_p is the identity operator for the photon degrees of freedom. The second line in Eq. (4) shows it coincides with the ensemble geometric phase for density matrices [29, 32–35]. However, here the reduced electron density matrix $\hat{\rho}_{el}$ is a mixed one due to light-matter entanglement produced by the cavity coupling. We emphasize that, while the mentioned references utilize periodic

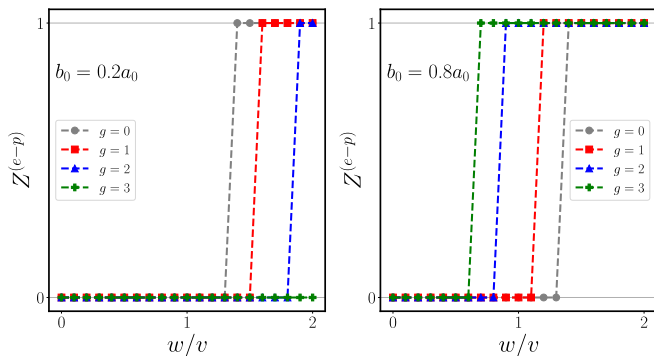


FIG. 3. Many-body light-matter topological marker at half-filling as a function of w/v for $g = 0, 1, 2, 3$ and $b_0 = 0.2a_0$ (left), $0.8a_0$ (right). Other parameters: $\hbar\omega_c/v = 1$, $N = 5$.

boundary conditions, we employ open boundary conditions, which is essential to deal with transport properties. As shown in Fig. 3, such a quantity is an integer also for open boundaries with the only difference being a shift in the topological transition point for a finite-size system.

Cavity-modified electronic transport — Having the exact light-matter eigenstates, we can study the electron transport properties in the presence of the cavity in the linear response regime. The electronic system (S) is assumed to be coupled to Left (L) and Right (R) leads (Fig. 1), as described by the Hamiltonian:

$$\hat{H} = \hat{H}_S + \hat{H}_L + \hat{H}_R + \hat{V}, \quad (5)$$

where \hat{H}_S has already been shown in Eq. (2). The lead Hamiltonians are $\hat{H}_\lambda = -t_\lambda \sum_{n=1}^{N_\lambda} \hat{d}_{\lambda,n+1}^\dagger \hat{d}_{\lambda,n} + \text{h.c.}$ with $\lambda \in \{L, R\}$. Note that we consider the limit of large-size leads, implying that their chemical potentials μ_λ are unaffected by the coupling to the finite-size chain. The coupling between system and leads reads:

$$\hat{V} = \left(\gamma_L \hat{c}_{1,A}^\dagger \hat{d}_{L,1} + \gamma_R \hat{c}_{N,B}^\dagger \hat{d}_{R,1} + \text{h.c.} \right), \quad (6)$$

where γ_λ are the coupling constants.

To determine the quantum transport, we have generalized the framework for interacting conductors derived by Meir and Wingreen [30] to account for quantum light-matter interaction. The current J flowing through the system in the steady state depends on the Green's functions through the formula:

$$J = \frac{ie}{2\hbar} \int d\epsilon \text{Tr} \{ [f_L(\epsilon)\Gamma^L - f_R(\epsilon)\Gamma^R] (G^r - G^a) \} + \text{Tr} \{ (\Gamma^L - \Gamma^R) G^< \}, \quad (7)$$

where f_λ represent Fermi-Dirac distribution of the lead λ with chemical potential μ_λ . The matrices Γ^λ depend on the retarded and advanced self-energy terms due to coupling to the corresponding lead, namely $\Gamma^\lambda =$

$i(\Sigma_\lambda^r - \Sigma_\lambda^a)$. The propagators $G^r, G^a, G^<$ are respectively the non-equilibrium retarded, advanced and lesser electronic Green functions of the system in the presence of both leads and light-matter interaction. It is important to note that the matrices involved in (7) have a dimension given by the system's electronic single-body Hilbert space. A detailed derivation of the Green functions and self-energies can be found in [13, 30, 36] and our Supplementary Material.

The non-equilibrium Green's functions satisfy the following equations [36–38]:

$$\begin{aligned} G^r &= g_0^r + g_0^r (\Sigma_{\text{leads}}^r + \Sigma_{\text{int}}^r) G^r, \\ G^a &= [G^r]^\dagger, \\ G^< &= G^r (\Sigma_{\text{leads}}^< + \Sigma_{\text{int}}^<) G^a. \end{aligned} \quad (8)$$

Here $g_0^r(\omega)$ denotes the electron's retarded Green functions of the system without light-matter interaction and without coupling to the leads. The retarded and lesser

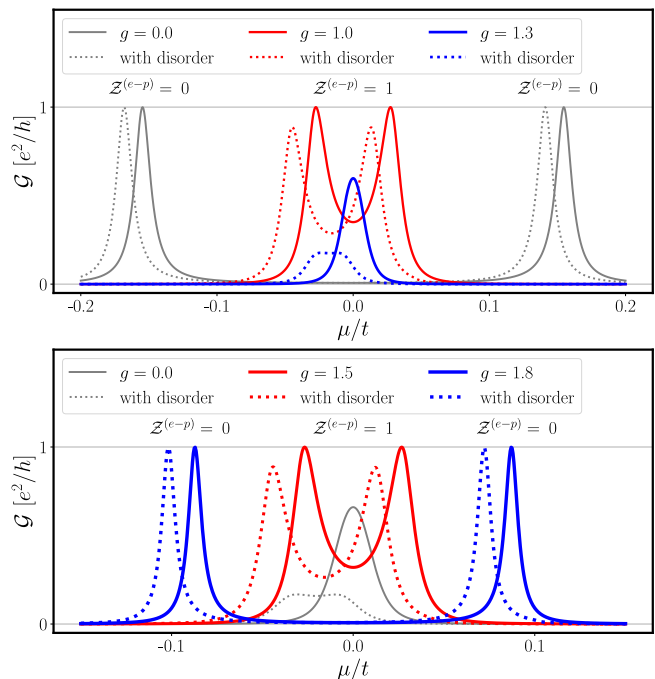


FIG. 4. Electron conductance $\mathcal{G}(\mu)$ calculated near the half-filling point ($\mu = 0$) versus μ/t with different values of the dimensionless coupling strength g for two scenarios (top and bottom panels) without (solid lines) or with (dotted lines) random electronic disorder with energy amplitude $W = 0.05t$. The value of the topological marker $Z^{(e-p)}$ for the peaks of conductance is indicated in the plot. Top: increasing the cavity coupling g reduces the gap between quantized conductance peaks and the quantization is eventually lost. Parameters: $v = 1.0t$, $w = 1.2t$, $b_0 = 0.8a_0$. Bottom: increasing the cavity coupling opens a gap and the conductance becomes quantized. Parameters $v = 0.6t$, $w = 1.4t$, $b_0 = 0.1a_0$. Common parameters for the two panels: $N = 6$, $\gamma_L = \gamma_R = 0.13t$, $\hbar\omega_c = 5.0t$, $t_L = t_R = t$.

self-energies due to leads $\Sigma_{\text{leads}}^{r,<}(\omega) = \Sigma_L^{r,<}(\omega) + \Sigma_R^{r,<}(\omega)$ are provided in the Supplementary Material, while $\Sigma_{\text{int}}^{r,<}$ arises from light-matter interaction. The latter in general depends on the number of electrons within the system *after* coupling to the leads, therefore on μ_L and μ_R . This term is often treated perturbatively and self-consistently, as discussed in references [36, 37]. Such dependence can be neglected in the weak tunneling limit between the systems and leads, i.e., $\gamma_{L,R}/t \ll N$ in Eq. (6). Under this approximation, $\Sigma_{\text{int}}^{r,<}$ can be derived exactly from (2). This procedure generates results that are non-perturbative with respect to light-matter interaction, but perturbative in the coupling to the leads. Detailed calculations are given in Supplementary Material.

In presence of a voltage bias V such that $\mu_{L,R} = \mu \pm V/2$, a current flows through the system. At zero temperature the linear conductance reads:

$$\mathcal{G} = \lim_{V \rightarrow 0} \frac{J}{V} = \frac{e^2}{h} \left| \text{Tr} \left[\frac{i}{4} \Gamma^p (G^r - G^a) - \frac{1}{4} \Gamma^m G^r \Gamma^m G^a \right] \right|, \quad (9)$$

where $\Gamma^{p,m} = \Gamma^L \pm \Gamma^R$. Note that we have omitted the dependence on the chemical potential in the mathematical notation for the sake of simplicity. The results are illustrated in Fig. 4 where two different scenarios ($g_v > g_w$ versus $g_v < g_w$) are reported in two corresponding panels (top and bottom, respectively). In the top panel, we consider the chain to be in a topologically trivial phase with $Z^{(e-p)} = 0$ in the absence of light-matter interaction ($g = 0$). In such a configuration, the states are delocalized over the finite-size chain leading to the observation of a quantized conductance e^2/h when the system chemical potential μ is properly aligned. Due to the electron-hole symmetry, two identical peaks are symmetrically located around the half-filling point. Increasing the cavity coupling reduces the gap between the two peaks, eventually producing a topological transition towards the non-trivial phase with $Z^{(e-p)} = 1$. Increasing enough g , the topological edge states becomes more and more localized producing an eventual loss of the conductance quantization. Note that the dotted curves correspond to the electron conductance in the presence of disorder. We have considered here an on-site electronic energy random disorder with an uniform probability distribution in the interval $[-W, W]$. In the figure, we have considered $W = 0.05t$. Since $2W$ is smaller than the energy gap between the conductance peaks for the $g = 0$ case, the effect of disorder is to produce a shift of the conductance peak energy with $Z^{(e-p)} = 0$, but its quantization holds. Instead, $2W$ is larger than the energy splitting for $g = 1$ and $g = 1.3$, resulting in a loss of quantization for $g = 1$ and a dramatic modification of the peak for $g = 1.3$. Note that we have calculated a large number of disorder random realizations (not shown) and the same qualitative picture is consistently observed, apart from quantitative variations.

The opposite scenario is achieved in the bottom panel

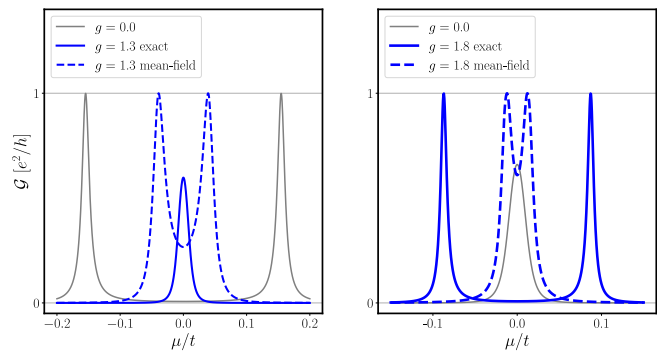


FIG. 5. Comparison between conductances calculated from exact diagonalization (solid line) and mean-field (dashed line). Same parameters as in Fig. 4.

where $g_v < g_w$. Here for no cavity coupling ($g = 0$), the SSH chain is topologically non-trivial with a non-quantized single conductance peak. Increasing the cavity coupling opens a gap and the conductance become quantized at the peaks. The conductance with disorder (dotted lines) shows a similar behavior as in the top panel. In the Supplementary Material, we have reported other examples of results for larger and smaller values of the disorder energy amplitude W .

In Fig. 5 we compare the conductance calculated with exact diagonalization to the predictions of mean-field theory, where the ground state of (2) is approximated as separable (no electron-photon entanglement), namely $|GS^{(e-p)}\rangle \simeq |\psi^{(e)}\rangle |\chi^{(p)}\rangle$. The latter is equivalent to consider a purely electronic model with hopping parameters v and w that are self-consistently renormalized by the photon field (for details see Supplementary Material). Our results show a breakdown of mean-field theory, which is due to the significant degree of light-matter entanglement shown in Fig. 2. In all scenarios, the entanglement significantly enhances the impact of the cavity quantum field on the electronic conductance.

Conclusions — In this Letter, we provided the first study of cavity-modified topology and transport beyond the single-particle picture and without adiabatic elimination of the photon degrees of freedom by exploiting an exact diagonalization approach. We focused our study on a paradigmatic topological 1D system, namely an SSH chain. We have introduced a novel topological many-body marker for the light-matter system, which is a generalization of the Zak phase, but that is valid for any arbitrary light-matter coupling and entanglement. Moreover, we have studied cavity-modified electron transport in the linear regime for finite-size chains by exploiting the many-body eigenstates, showing the crucial role of light-matter entanglement.

We acknowledge financial support from the French agency ANR through the project CaVdW (ANR-21-CE30-0056-0) and from the Israeli Council for Higher

-
- [1] P. Forn-Díaz, L. Lamata, E. Rico, J. Kono, and E. Solano, Ultrastrong coupling regimes of light-matter interaction, *Reviews of Modern Physics* **91** (2019).
- [2] A. F. Kockum, A. Miranowicz, S. D. Liberato, S. Savasta, and F. Nori, Ultrastrong coupling between light and matter, *Nature Reviews Physics* **1**, 19 (2019).
- [3] F. J. Garcia-Vidal, C. Ciuti, and T. W. Ebbesen, Manipulating matter by strong coupling to vacuum fields, *Science* **373** (2021).
- [4] F. Schlawin, D. M. Kennes, and M. A. Sentef, Cavity quantum materials, *Applied Physics Reviews* **9**, 011312 (2022).
- [5] J. Keller, G. Scalari, S. Cibella, C. Maissen, F. Appugliese, E. Giovine, R. Leoni, M. Beck, and J. Faist, Few-Electron Ultrastrong Light-Matter Coupling at 300 GHz with Nanogap Hybrid LC Microcavities, *Nano Letters* **17**, 7410 (2017).
- [6] G. Scalari, C. Maissen, D. Turcinkova, D. Hagenmuller, S. D. Liberato, C. Ciuti, C. Reichl, D. Schuh, W. Wegscheider, M. Beck, and J. Faist, Ultrastrong Coupling of the Cyclotron Transition of a 2D Electron Gas to a THz Metamaterial, *Science* **335**, 1323 (2012).
- [7] G. L. Paravicini-Bagliani, F. Appugliese, E. Richter, F. Valmorra, J. Keller, M. Beck, N. Bartolo, C. Rössler, T. Ihn, K. Ensslin, C. Ciuti, G. Scalari, and J. Faist, Magneto-transport controlled by Landau polariton states, *Nature Physics* **15**, 186 (2018).
- [8] Y. Ashida, A. İmamoğlu, and E. Demler, Cavity Quantum Electrodynamics with Hyperbolic van der Waals Materials, *Physical Review Letters* **130** (2023).
- [9] M. A. Sentef, M. Ruggenthaler, and A. Rubio, Cavity quantum-electrodynamical polaritonically enhanced electron-phonon coupling and its influence on superconductivity, *Science Advances* **4** (2018).
- [10] J. B. Curtis, Z. M. Raines, A. A. Allocca, M. Hafezi, and V. M. Galitski, Cavity Quantum Eliashberg Enhancement of Superconductivity, *Physical Review Letters* **122** (2019).
- [11] F. Schlawin, A. Cavalleri, and D. Jaksch, Cavity-Mediated Electron-Photon Superconductivity, *Physical Review Letters* **122** (2019).
- [12] C. Ciuti, Cavity-mediated electron hopping in disordered quantum Hall systems, *Physical Review B* **104** (2021).
- [13] G. Arwas and C. Ciuti, Quantum electron transport controlled by cavity vacuum fields, *Physical Review B* **107** (2023).
- [14] V. Rokaj, J. Wang, J. Sous, M. Penz, M. Ruggenthaler, and A. Rubio, Weakened Topological Protection of the Quantum Hall Effect in a Cavity, *Physical Review Letters* **131** (2023).
- [15] L. Winter and O. Zilberberg, Fractional quantum Hall edge polaritons, [arXiv:2308.12146](https://arxiv.org/abs/2308.12146) (2023).
- [16] O. Dmytruk and M. Schirò, Controlling topological phases of matter with quantum light, *Communications Physics* **5** (2022).
- [17] J. Li, L. Schamriß, and M. Eckstein, Effective theory of lattice electrons strongly coupled to quantum electromagnetic fields, *Physical Review B* **105** (2022).
- [18] D. Shaffer, M. Claassen, A. Srivastava, and L. H. Santos, Entanglement and Topology in Su-Schrieffer-Heeger Cavity Quantum Electrodynamics, [arXiv:2308.08588](https://arxiv.org/abs/2308.08588) (2023).
- [19] D.-P. Nguyen, G. Arwas, Z. Lin, W. Yao, and C. Ciuti, Electron-Photon Chern Number in Cavity-Embedded 2D Moiré Materials, *Physical Review Letters* **131** (2023).
- [20] Z. Bacciconi, G. M. Andolina, and C. Mora, Topological protection of Majorana polaritons in a cavity, [arXiv:2309.07278](https://arxiv.org/abs/2309.07278) (2023).
- [21] Z. Lin, C. Xiao, D.-P. Nguyen, G. Arwas, C. Ciuti, and W. Yao, Remote gate control of topological transitions in moiré superlattices via cavity vacuum fields, *Proceedings of the National Academy of Sciences* **120** (2023).
- [22] C. B. Dag and V. Rokaj, Cavity Induced Topology in Graphene, [arXiv:2311.02806](https://arxiv.org/abs/2311.02806) (2023).
- [23] F. Appugliese, J. Enkner, G. L. Paravicini-Bagliani, M. Beck, C. Reichl, W. Wegscheider, G. Scalari, C. Ciuti, and J. Faist, Breakdown of topological protection by cavity vacuum fields in the integer quantum Hall effect, *Science* **375**, 1030 (2022).
- [24] G. Jarc, S. Y. Mathengattil, A. Montanaro, F. Giusti, E. M. Rigoni, R. Sergo, F. Fassoli, S. Winnerl, S. Dal Zilio, D. Mihailovic, P. Prelovšek, M. Eckstein, and D. Fausti, Cavity-mediated thermal control of metal-to-insulator transition in 1T-TaS₂, *Nature* **622**, 487–492 (2023).
- [25] G. M. Andolina, F. M. D. Pellegrino, V. Giovannetti, A. H. MacDonald, and M. Polini, Cavity quantum electrodynamics of strongly correlated electron systems: A no-go theorem for photon condensation, *Physical Review B* **100** (2019).
- [26] D. Guerci, P. Simon, and C. Mora, Superradiant Phase Transition in Electronic Systems and Emergent Topological Phases, *Phys. Rev. Lett.* **125**, 257604 (2020).
- [27] Z. Bacciconi, G. M. Andolina, T. Chanda, G. Chiriaco, M. Schirò, and M. Dalmonte, First-order photon condensation in magnetic cavities: A two-leg ladder model, *SciPost Physics* **15** (2023).
- [28] I. Gilardoni, F. Becca, A. Marrazzo, and A. Parola, Real-space many-body marker for correlated \mathbb{Z}_2 topological insulators, *Physical Review B* **106** (2022).
- [29] P. Mognini and N. R. Cooper, Topological phase transitions at finite temperature, *Physical Review Research* **5** (2023).
- [30] Y. Meir and N. S. Wingreen, Landauer formula for the current through an interacting electron region, *Physical Review Letters* **68**, 2512 (1992).
- [31] R. Resta, Quantum-Mechanical Position Operator in Extended Systems, *Physical Review Letters* **80**, 1800 (1998).
- [32] C.-E. Bardyn, L. Wawer, A. Altland, M. Fleischhauer, and S. Diehl, Probing the Topology of Density Matrices, *Physical Review X* **8** (2018).
- [33] C. D. Mink, M. Fleischhauer, and R. Unanyan, Absence of topology in Gaussian mixed states of bosons, *Physical Review B* **100** (2019).
- [34] R. Unanyan, M. Kiefer-Emmanouilidis, and M. Fleischhauer, Finite-Temperature Topological Invariant for Interacting Systems, *Physical Review Letters* **125** (2020).
- [35] L. Wawer and M. Fleischhauer, Chern number and Berry curvature for Gaussian mixed states of fermions, *Physical Review B* **104** (2021).
- [36] S. Datta, *Electronic Transport in Mesoscopic Systems* (Cambridge University Press, 1995).

- [37] K. S. Thygesen and A. Rubio, Conserving GW scheme for nonequilibrium quantum transport in molecular contacts, [Physical Review B](#) **77** (2008).
- [38] P. I. Arseev, On the nonequilibrium diagram technique: derivation, some features, and applications, [Physics-Uspekhi](#) **58**, 1159–1205 (2015).

Supplementary Material for the article: “Electron conductance of a cavity-embedded topological 1D chain”

Danh-Phuong Nguyen, Geva Arwas, and Cristiano Ciuti
Université Paris Cité, CNRS, Matériaux et Phénomènes Quantiques, 75013 Paris, France
 (Dated: March 1, 2024)

I. GREEN'S FUNCTIONS

While employing the non-equilibrium Green's function formalism, we will use the symbols ' r ' and ' a ' to denote retarded and advanced Green's functions respectively. Moreover ' $<$ ' and ' $>$ ' will refer to lesser and greater Green's functions respectively. We will consider four different cases depending on the presence (or not) of leads and of a cavity. In particular, we will adopt the following notations for the Green's functions of the system only: g_0 for the case without leads, without cav-

$$g_{ab}^r(\omega, N_e) = \sum_{\xi \in \mathcal{S}_{N_e+1}} \frac{\langle GS, N_e | \hat{c}_a | \xi, N_e + 1 \rangle \langle \xi, N_e + 1 | \hat{c}_b^\dagger | GS, N_e \rangle}{\omega - \omega_{\xi, N_e+1} + \omega_{GS, N_e} + i\eta} + \sum_{\xi \in \mathcal{S}_{N_e-1}} \frac{\langle GS, N_e | \hat{c}_b^\dagger | \xi, N_e - 1 \rangle \langle \xi, N_e - 1 | \hat{c}_a | GS, N_e \rangle}{\omega - \omega_{GS, N_e} + \omega_{\xi, N_e-1} + i\eta}. \quad (\text{S.1})$$

The expression (S.1) is known as Lehmann representation. If we denote $g_0^r(\omega, N_e) = g_0^r(\omega)$ as the retarded Green function for the non-interacting case, then the retarded self-energy term $\Sigma_{\text{int}}^r(\omega, N_e)$ is defined as:

$$\Sigma_{\text{int}}^r(\omega, N_e) = [g_0^r(\omega)]^{-1} - [g^r(\omega, N_e)]^{-1}. \quad (\text{S.2})$$

In order to describe the effect of two leads on the system, we consider the Hamiltonian:

$$\hat{\mathcal{H}} = \hat{\mathcal{H}}_S + \hat{\mathcal{H}}_{\text{leads}} + \hat{V}, \quad (\text{S.3})$$

with $\hat{\mathcal{H}}_{\text{leads}} = \sum_{n, \lambda=L, R} t_\lambda \hat{d}_{\lambda, n+1}^\dagger \hat{d}_{\lambda, n}$ and the tunneling term $\hat{V} = \hat{v} + \hat{v}^\dagger$ with $\hat{v} = \gamma_L \hat{c}_{1,A}^\dagger \hat{d}_{L,1} + \gamma_R \hat{c}_{N,B}^\dagger \hat{d}_{R,1}$. In the non-interacting case, the single-body retarded Green function for the system and leads can be employed to simplify the problem: $\tilde{G}_0^r(\omega) = (\omega - \hat{\mathcal{H}} + i\eta)^{-1}$. More specifically, its block form is expressed as:

$$\begin{aligned} \tilde{G}_0^r(\omega) &= \begin{pmatrix} \omega - \hat{\mathcal{H}}_S + i\eta & -\hat{v} \\ -\hat{v}^\dagger & \omega - \hat{\mathcal{H}}_{\text{leads}} + i\eta \end{pmatrix}^{-1} \\ &= \begin{pmatrix} [g_{0,S}^r]^{-1}(\omega) & -\hat{v} \\ -\hat{v}^\dagger & [g_{0,\text{leads}}^r]^{-1}(\omega) \end{pmatrix}^{-1}, \end{aligned} \quad (\text{S.4})$$

where $g_{0,S}^r$ and $g_{0,\text{leads}}^r$ represent the retarded Green functions of the system and the leads when they are not coupled. The Green function for the system is obtained

ity; g without leads, with cavity; G_0 with leads, without cavity; G with leads, with cavity. While describing both system and leads, the Green functions will be denoted as $\tilde{g}_0, \tilde{g}, \tilde{G}_0$ and \tilde{G} .

The system Hamiltonian $\hat{\mathcal{H}}_S$ described in the main manuscript conserves the number N_e of fermionic particles. Therefore, the exact eigenstates have the form $|\chi, N_e\rangle$ and energies ϵ_{χ, N_e} where χ labels eigenstates in the N_e -electron eigenspace \mathcal{S}_{N_e} . The retarded Green's function matrix can be expressed in terms of such many-body eigenstates as follows:

through block matrix inversion:

$$\begin{aligned} G_{0,S}^r(\omega) &= g_{0,S}^r(\omega) [1 - \hat{v} g_{0,\text{leads}}^r(\omega) \hat{v}^\dagger g_{0,S}^r(\omega)]^{-1} \\ &= g_{0,S}^r(\omega) [1 - \Sigma_{\text{leads}}^r(\omega) g_{0,S}^r(\omega)]^{-1}. \end{aligned} \quad (\text{S.5})$$

In this context, the retarded self-energies induced by leads L, R are defined as $\Sigma_{\text{leads}}^r(\omega) = \hat{v} g_{0,\text{leads}}^r(\omega) \hat{v}^\dagger = \hat{v} g_{0,L}^r(\omega) \hat{v}^\dagger + \hat{v} g_{0,R}^r(\omega) \hat{v}^\dagger = \Sigma_L^r(\omega) + \Sigma_R^r(\omega)$. They read:

$$\begin{aligned} \Sigma_L^r(\omega) &= -\gamma_L^2 / t_L \exp(ik_L) |1, A\rangle \langle 1, A|, \\ \Sigma_R^r(\omega) &= -\gamma_R^2 / t_R \exp(ik_R) |N, B\rangle \langle N, B|, \end{aligned} \quad (\text{S.6})$$

with $\omega = -2t_\lambda \cos(k_\lambda)$. The states $|1, A\rangle$ and $|N, B\rangle$ are single-body states localized respectively at the beginning and end of the SSH chain. Another relevant quantity is described by the matrix $\Gamma_\lambda = i[\Sigma_\lambda^r - (\Sigma_\lambda^r)^\dagger]$, which, as will see, appears in the conductance formula. These matrices depend on the lead spectral functions $\Gamma_\lambda(\omega) = \hat{v} A_\lambda(\omega) \hat{v}^\dagger$. This formula can be exploited to calculate the lesser self-energies, which are defined in the same manner, namely $\Sigma_\lambda^<(\omega) = \hat{v} g_{0,\lambda}^< \hat{v}^\dagger$. They can be rewritten as

$$\Sigma_\lambda^<(\omega) = i f_{\mu_\lambda}(\omega) \hat{v} A(\omega) \hat{v}^\dagger = i f_{\mu_\lambda}(\omega) \Gamma_\lambda(\omega), \quad (\text{S.7})$$

with f_{μ_λ} the Fermi-Dirac distribution corresponding to the chemical potential μ_λ .

With a coupling to a cavity mode, we can prove that non-equilibrium Green functions \tilde{G} satisfy the equation:

$$\tilde{G}(\omega) = \tilde{g}(\omega) + \tilde{g}(\omega) V \tilde{G}(\omega), \quad (\text{S.8})$$

where \tilde{g} , \tilde{G} , V are block matrices:

$$\begin{aligned}\tilde{G} &= \begin{pmatrix} \tilde{G}^r & \tilde{G}^< \\ 0 & \tilde{G}^a \end{pmatrix}, \\ V &= \begin{pmatrix} \hat{V} & 0 \\ 0 & \hat{V} \end{pmatrix}.\end{aligned}\quad (\text{S.9})$$

Note that \hat{V} in the second formula of (S.9) is written in single-body formalism, and \tilde{g} is defined in the same way as \tilde{G} . Since we only consider the correlators within the system S , equation (S.8) could be re-written as $\tilde{G} = \tilde{g} + \tilde{g}V\tilde{g} + \tilde{g}V\tilde{g}V\tilde{G}$. After matrix multiplication, for the system S we get:

$$\begin{aligned}G_S^r &= g_S^r + g_S^r \Sigma_{\text{leads}}^r G_S^r, \\ G_S^< &= G_S^r (\Sigma_{\text{leads}}^< + [g_S^r]^{-1} g_S^< [g_S^a]^{-1}) G^a,\end{aligned}\quad (\text{S.10})$$

where the self-energies $\Sigma_{\text{leads}}^{r,<}$ are defined above. The first expression of (S.10) can be rewritten as $[G_S^r]^{-1} = [g_S^r]^{-1} - \Sigma_{\text{leads}}^r = [g_{0S}^r]^{-1} - \Sigma_{\text{int}}^r - \Sigma_{\text{leads}}^r$. The second formula involving lesser Green function can be proven by the relation $g_S^< = g_S^r \Sigma_{\text{int}}^< g_S^a$.

II. LINEAR CONDUCTANCE AT ZERO TEMPERATURE

From this point forward, we refer only to the system's Green functions, so we omit the S in the expressions in order to simplify the notation.

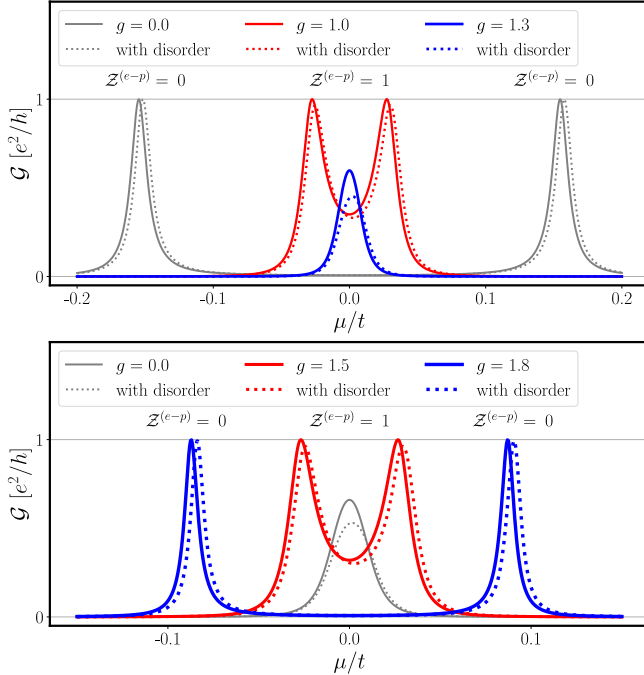


FIG. S1. Same conductance curves as in Fig. 4 of the main manuscript, but with the disorder amplitude $W = 0.015t$.

Meir and Wingreen derived a Landauer formula for a strongly interacting region, namely

$$\begin{aligned}J &= \frac{ie}{2\hbar} \int d\epsilon \text{Tr}\{[f_L(\epsilon)\Gamma^L - f_R(\epsilon)\Gamma^R] (G^r - G^a)\} \\ &\quad + \text{Tr}\{(\Gamma^L - \Gamma^R) G^<\},\end{aligned}\quad (\text{S.11})$$

where J is the current flowing through the system, and $f_{L,R}(\epsilon) = f(\mu \pm V/2, \epsilon)$ is the Fermi-Dirac distributions with chemical potential $\mu \pm V/2$ for the left and right lead, respectively. $G^{r,a,<}$ are the system's Green functions, accounting for both leads and light-matter interaction. They can be dealt using the Keldysh formalism. In the following, we will restrict to the linear response regime (i.e. $V \rightarrow 0$) and in the limit of zero temperature. In the case of *dynamical* decoupling between system and leads, we precisely compute $\Sigma_{\text{int}}^r(\omega, N_e)$ from (S.2) by minimizing $\hat{\mathcal{H}} - \mu\hat{N}$, where \hat{N} is the fermionic number operator. In the limit of weak tunneling between leads and system, we assume that $\Sigma_{\text{int}}^{r,<}$ is unaffected. In the linear conductance regime we have the following relations:

$$\begin{aligned}f_{L,R}(\epsilon) &= f(\mu, \epsilon) \pm \frac{V}{2} \frac{\partial f}{\partial \mu}(\mu, \epsilon), \\ \Sigma_{\text{leads}}^<(\epsilon) &= if(\mu, \epsilon) [\Gamma_L(\epsilon) + \Gamma_R(\epsilon)] \\ &\quad + i \frac{V}{2} \frac{\partial f}{\partial \mu}(\mu, \epsilon) [\Gamma_L(\epsilon) - \Gamma_R(\epsilon)].\end{aligned}\quad (\text{S.12})$$

At zero temperature, $\partial f/\partial \mu(\mu, \epsilon) = -\delta(\epsilon - \mu)$. The conductance is calculated as $\mathcal{G} = \lim_{V \rightarrow 0} [J(V) - J(0)]/V$,

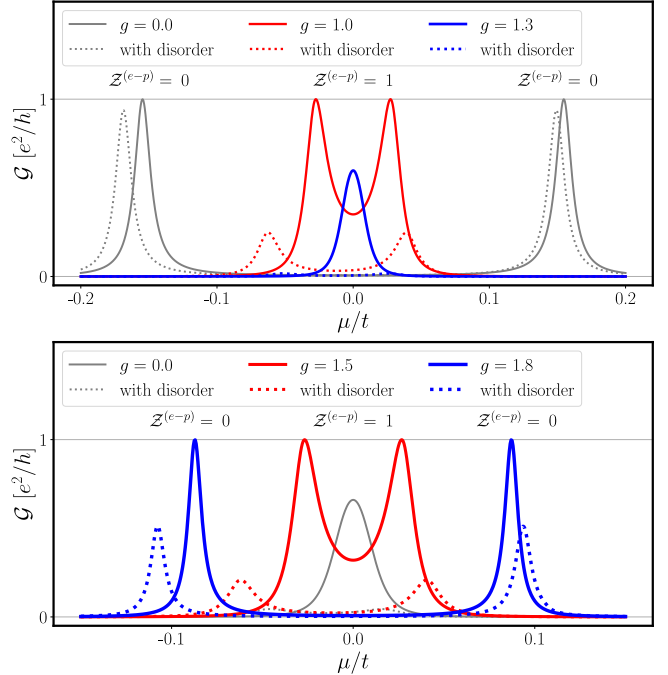


FIG. S2. Same conductance curves as in Fig. 4 of the main manuscript, but with the disorder amplitude $W = 0.15t$.

resulting in:

$$\mathcal{G} = \frac{e^2}{h} \left| \text{Tr} \left[\frac{i}{4} \Gamma^p (G^r - G^a) - \frac{1}{4} \Gamma^m G^r \Gamma^m G^a \right] \right|. \quad (\text{S.13})$$

In the above equation, we define $\Gamma^{p,m} = \Gamma^L \pm \Gamma^R$ and omit the dependence on the chemical potential for clarity.

III. ADDITIONAL RESULTS WITH DISORDER

Here we show conductance curves as in Fig. 4 of the main manuscript, but with different values of the disorder amplitude W , namely $W = 0.015t$ in Fig. S1 and $W =$

$0.15t$ for Fig. S2.

IV. MEAN-FIELD THEORY

Here we provide details about the mean-field theory obtained by assuming the separable ansatz $|GS^{(e-p)}\rangle = |\psi^{(e)}\rangle |\chi^{(p)}\rangle$ for the electron-photon ground state. This approximation (no light-matter entanglement) yields two effective Hamiltonians, namely $\hat{\mathcal{H}}_e^{\text{eff}} = \langle \chi^{(p)} | \hat{\mathcal{H}}_S | \chi^{(p)} \rangle$ for the electronic system and $\hat{\mathcal{H}}_p^{\text{eff}} = \langle \psi^{(e)} | \hat{\mathcal{H}}_S | \psi^{(e)} \rangle$ for the photonic one. To obtain $|\psi^{(e)}\rangle$ and $|\chi^{(p)}\rangle$, we solve in a self-consistent manner the ground states for the two Hamiltonians. The two effective Hamiltonians read:

$$\begin{aligned} \hat{\mathcal{H}}_e^{\text{eff}} &= \hbar\omega_c \langle \chi^{(p)} | \hat{a}^\dagger \hat{a} | \chi^{(p)} \rangle + \left(v \langle \chi^{(p)} | e^{-ig_v(\hat{a} + \hat{a}^\dagger)} | \chi^{(p)} \rangle \sum_{n=1}^N \hat{c}_{n,B}^\dagger \hat{c}_{n,A} + w \langle \chi^{(p)} | e^{+ig_w(\hat{a} + \hat{a}^\dagger)} | \chi^{(p)} \rangle \sum_{n=1}^{N-1} \hat{c}_{n+1,A}^\dagger \hat{c}_{n,B} + \text{h.c.} \right), \\ \hat{\mathcal{H}}_p^{\text{eff}} &= \hbar\omega_c \hat{a}^\dagger \hat{a} + \left(v e^{-ig_v(\hat{a} + \hat{a}^\dagger)} \sum_{n=1}^N \langle \psi^{(e)} | \hat{c}_{n,B}^\dagger \hat{c}_{n,A} | \psi^{(e)} \rangle + w e^{+ig_w(\hat{a} + \hat{a}^\dagger)} \sum_{n=1}^{N-1} \langle \psi^{(e)} | \hat{c}_{n+1,A}^\dagger \hat{c}_{n,B} | \psi^{(e)} \rangle + \text{h.c.} \right). \end{aligned} \quad (\text{S.14})$$

Note that in the mean-field approximation the impact on the electronic part is essentially a renormalization of the parameters v and w . Indeed, we have the renormalized parameters $\tilde{v} = v \langle \chi^{(p)} | e^{-ig_v(\hat{a} + \hat{a}^\dagger)} | \chi^{(p)} \rangle$ and $\tilde{w} = w \langle \chi^{(p)} | e^{+ig_w(\hat{a} + \hat{a}^\dagger)} | \chi^{(p)} \rangle$.